Supplement of Nat. Hazards Earth Syst. Sci., 20, 981–997, 2020
https://doi.org/10.5194/nhess-20-981-2020-supplement
© Author(s) 2020. This work is distributed under
the Creative Commons Attribution 4.0 License.

Natural Hazards and Earth System Sciences
Open Access

Supplement of

Urban pluvial flood risk assessment – data resolution and spatial scale when developing screening approaches on the microscale

Roland Löwe and Karsten Arnbjerg-Nielsen

Correspondence to: Roland Löwe (rolo@env.dtu.dk)

The copyright of individual parts of the supplement might differ from the CC BY 4.0 License.

S1 Relationship between impervious area and building area in the case study

Figure S 1 illustrates scatterplots of total impervious area vs. total building area after aggregating the original polygon data to grids with varying pixel sizes.

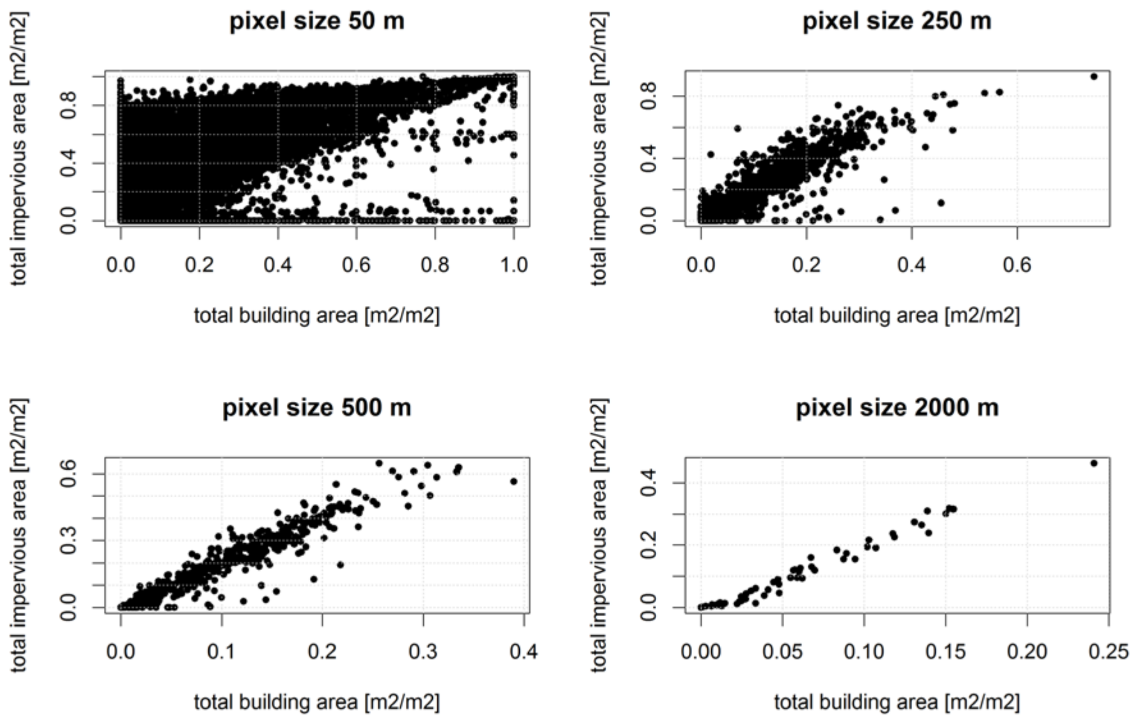

Figure S 1. Scatterplots of impervious area vs. total building area after aggregation to different pixel sizes.

S2 Regression coefficients for predicting imperviousness ratios in 2D flood simulations

For 2D flood simulation, impervious areas were calculated based on aggregated building datasets using the regression relationship below. The coefficients were derived with a raster resolution of 400m and the units of both input data and predicted impervious area are [m^2/m^2]. Building types are summarized in Table S 1. Footprint areas for utility buildings were not considered in this relationship because the associate coefficients were consistently found to be insignificant.

$$A_{imp} = 2.08A_{bf,commercial} + 1.45A_{bf,cultural} + 1.64A_{bf,industrial} + 0.23A_{bf,agricultural} + 1.55A_{bf,public\ residence} + 1.99A_{bf,public\ services} + 2.22A_{bf,residential\ block} + 1.93A_{bf,residential\ detached} + 2.08A_{bf,residential\ rowhouse} + 1.24A_{bf,general\ services} \quad (1)$$

S3 Infiltration rates for 2D flood simulations

Figure S 2 illustrates maps of infiltration rates that were used to parameterize the 2D flood simulations in the baseline simulation and for a situation where the building data were aggregated to a resolution of 500m.

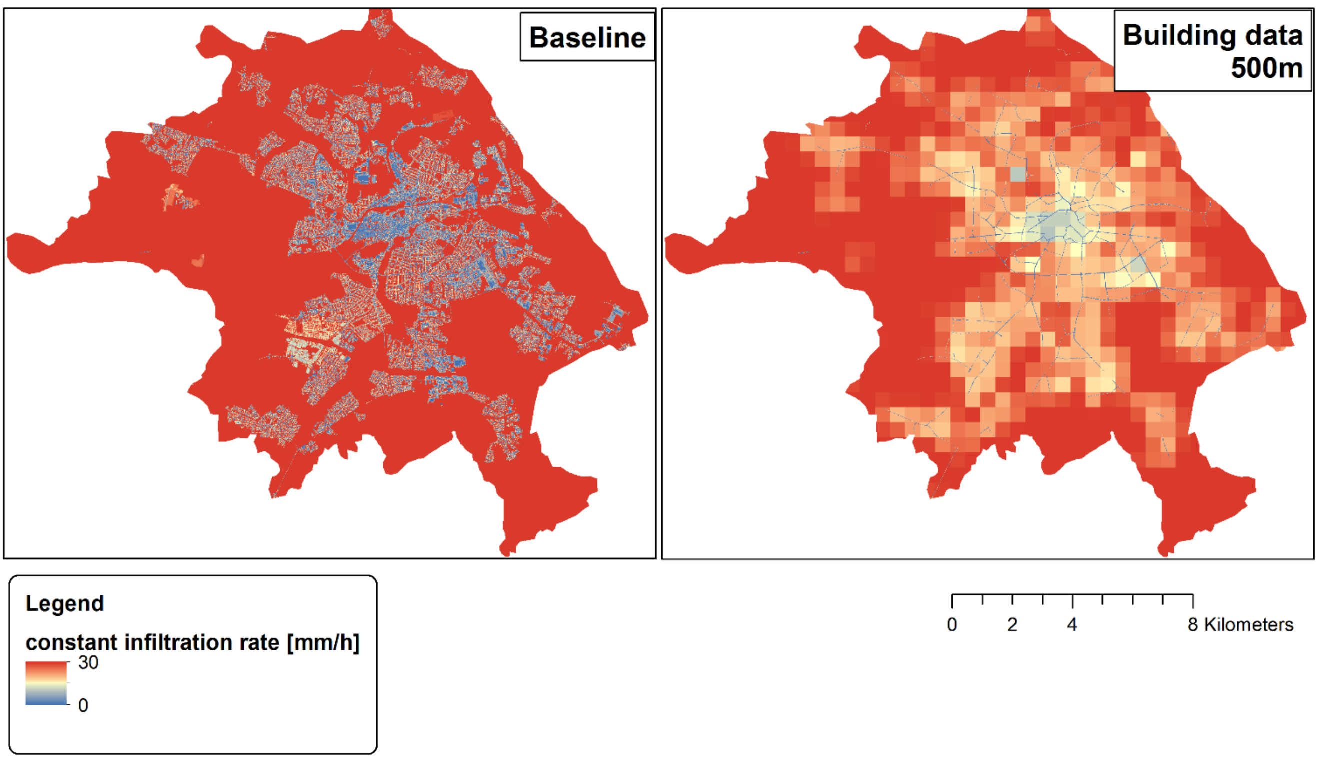

Figure S 2. Infiltration rates $f_t(1 - IS)$ applied in 2D flood simulation considering the baseline dataset (left) and infiltration rates derived from a building dataset that was aggregated to a resolution of 500m (right).

S4 Case study building types

Table S 1. Case study building types and assignment to building classes in the two damage frameworks

Type case study	Damage class in this study	Name in Olsen et al. (2015)	Name in Beckers et al. (2013)
Residential block	Residential	Residential	Residential
Public residence	Residential	Residential	Residential
Residential row-house	Residential	Residential	Residential
Detached residential	Residential	Residential	Residential
Commercial (warehouse, shopping malls and similar)	Commercial	Commercial	Industry and business area
Industrial	Commercial	Commercial	Industry and business area
Commercial services (kiosk, restaurants, etc.)	Commercial	Commercial	Industry and business area
Utility (water treatment facility, transformer building, etc.)	Commercial	Commercial	Industry and business area
Cultural	Public	Public Institution	Governmental utilization
Public services (schools, police, medical facilities, etc.)	Public	Public Institution	Governmental utilization
Agricultural	Commercial with damages from Olsen et al. (2015), excluded otherwise	Commercial	Excluded

S5 Subdivision of the case study area for cross validation in damage regression

Figure S 3 illustrates how our case study area was subdivided into cells with an edge length of 2000m when performing cross-validation during damage regression. Different colours indicate different subareas. Areas were damages were zero were excluded from the dataset. These areas were typically located beyond the watershed and thus not considered in the 2D flood simulation (c.f. Figure S 2).

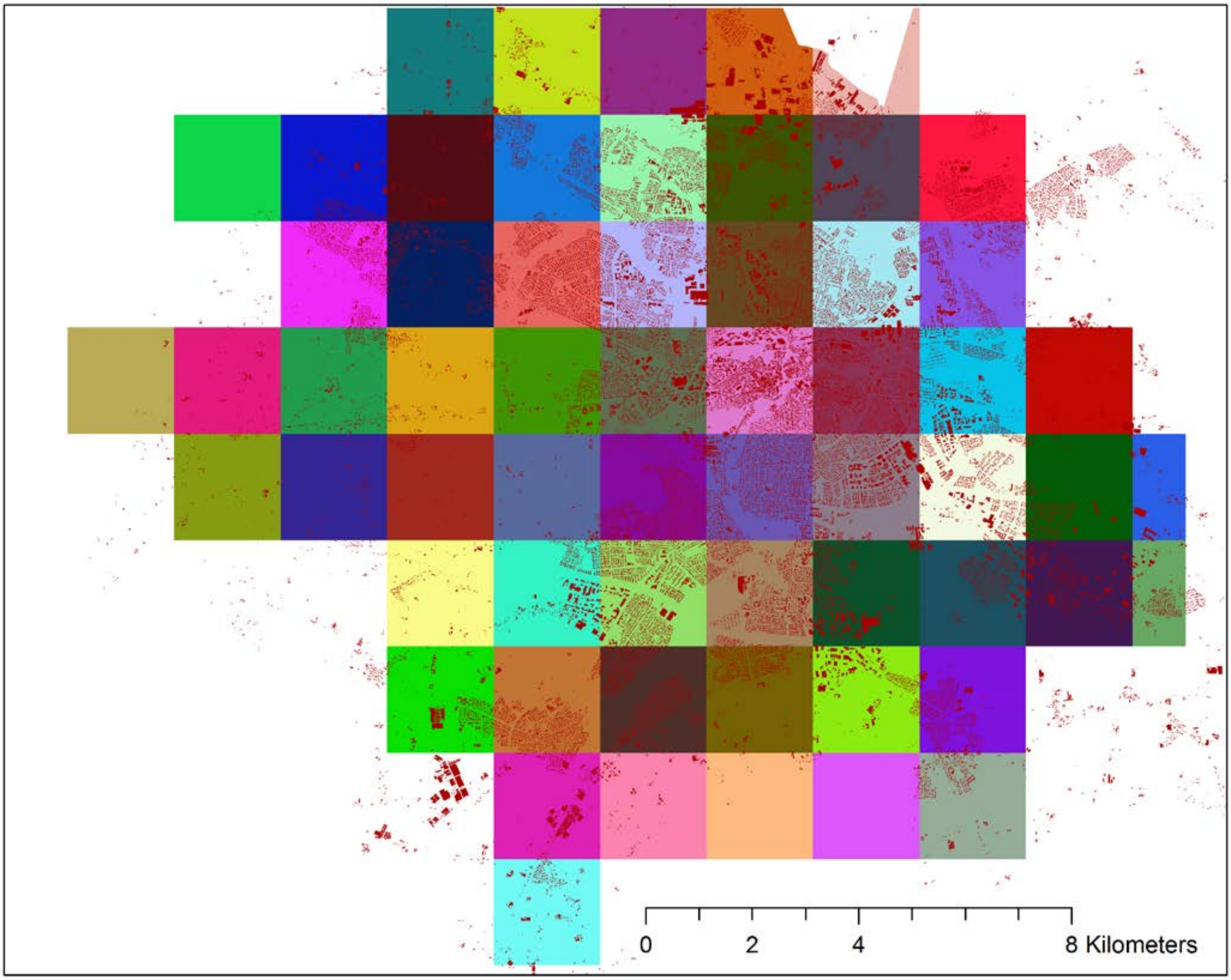

Figure S 3. Subdivision of the case study area into cells of 2000x2000m for cross validation during damage regression.

S6 Data transformation in flood damage regression

Figure S 4 and Figure S 5 show scatterplots of flood damages D (derived using the damage frameworks of Olsen et al. (2015) and Beckers et al. (2013)) vs. total flooded building areas A_{bf} (aggregated over all building types).

The plots are shown for a data resolution Δx_{fit} of 1000m and flooded building areas were derived using rasterized building data with a resolution Δx_b of 200m. The different columns illustrate scatter plots obtained for return periods of 20 and 100 years, while varying data transformations where applied in each row of the figures:

- No transformation (top row)
- $\sqrt{D} \sim \sqrt{A_{bf}}$: squareroot-squareroot-transformation (centre row)
- $\log(D + p_1) \sim \log(A_{bf} + p_2)$: log-log-transformation (bottom row). The coefficients p_1 and p_2 were included to handle zero values and were selected in such a way that the correlation between transformed flood damages and transformed flooded building areas was maximized ($p_1 = 0.05$,$p_2 = 1$).

Both figures suggest that the data transformations linearized the relationship between flooded building area and flood damages. The highest correlation between input and output was obtained when applying a log-log-transform. However, when computing flooded building areas based on rasterized building data (here with a resolution Δx_b of 200m), a non-zero flooded building area would be identified in some pixels where the “observed” flood damages were zero. The log-log-transform would amplify the influence of such outliers in the regression, which is not desirable. In addition, offset coefficients p_1 and p_2 need to be introduced when applying a log-log-transform to be able to handle pixels where flood damages or flooded building area are zero. As a result, the regression model fitted to log-log-transformed data is not guaranteed to predict a flood damage of 0 in pixels where the flooded building area is 0. This effect is not desirable as well. We have therefore considered a squareroot-squareroot transform in our work.

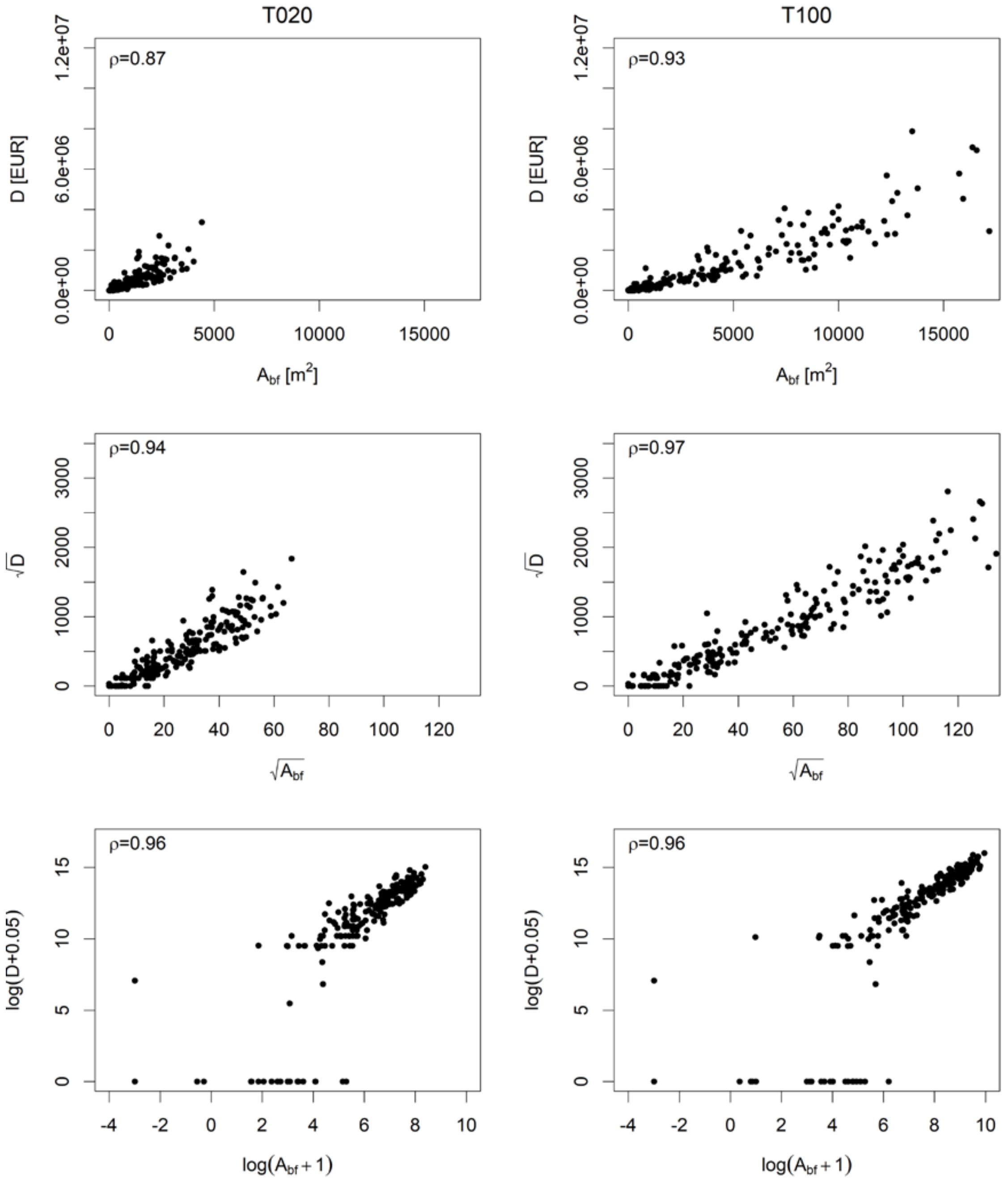

Figure S 4. Scatterplots of flood damages derived using the damage framework of (Olsen et al., 2015) versus total flooded building area (derived based on rasterized building data with a resolution of Δx_b of 200m). Columns show plots for events with return periods of T=20 years (left) and T=100 years (right). Rows show plots where different data transformations were applied (top-no transformation, middle: sqrt-sqrt-transformation, bottom: log-log-transformation). Plots are shown for a data resolution Δx_{fit} of 1000m. Correlations ρ are shown as text in each figure.

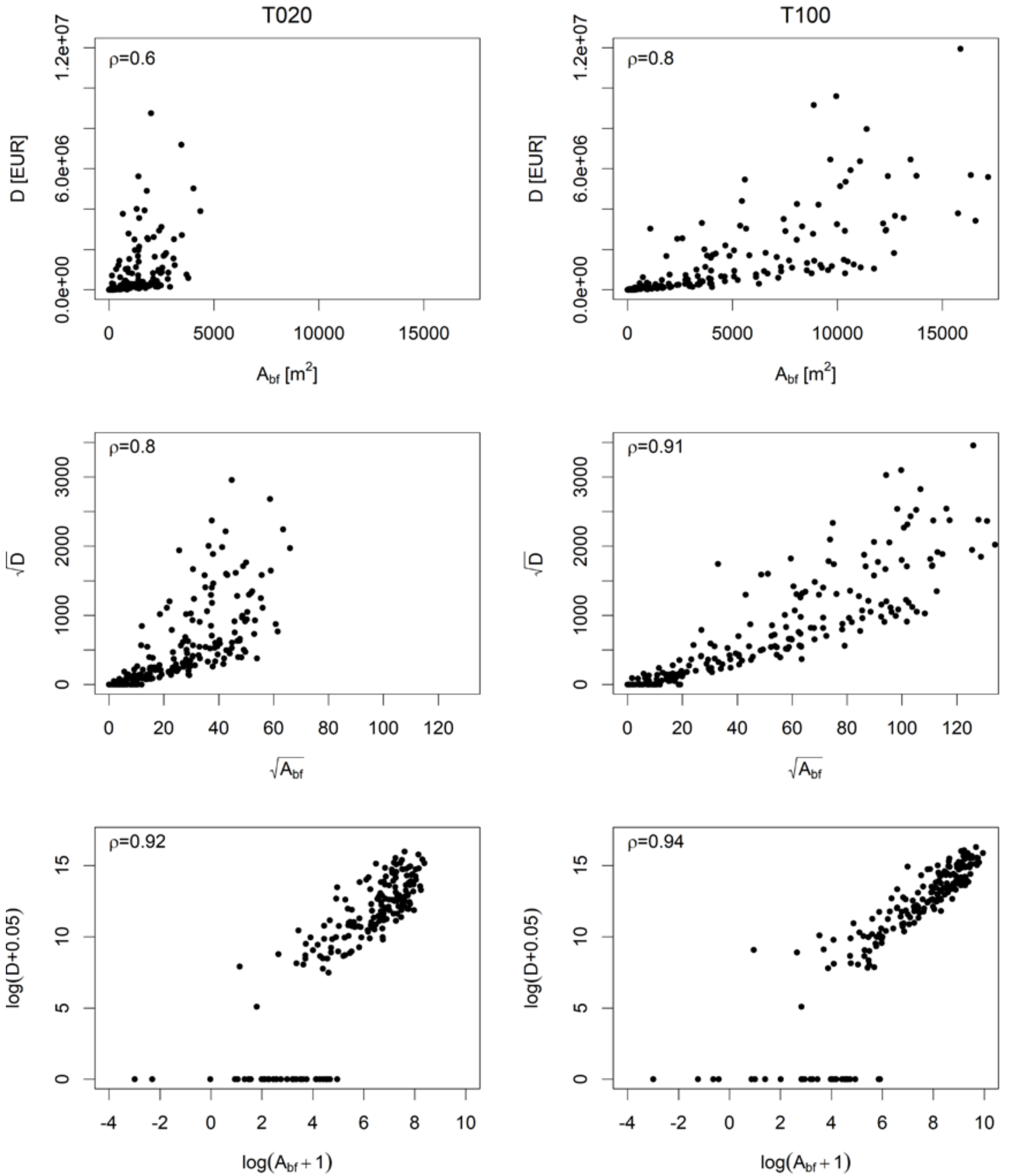

Figure S 5. Scatterplots of flood damages derived using the damage framework of (Beckers et al., 2013) versus total flooded building area (derived based on rasterized building data with a resolution of Δx_b of 200m). Columns show plots for events with return periods of T=20 years (left) and T=100 years (right). Rows show plots where different data transformations were applied (top-no transformation, middle: sqrt-sqrt-transformation, bottom: log-log-transformation). Plots are shown for a data resolution Δx_{fit} of 1000m. Correlations ρ are shown as text in each figure.

S7 Total damage estimates in damage regression

Figure S 4 illustrates the variation of damage ratios DR_{tot} as a function of the data resolution applied when estimating parameters of the damage regression models.

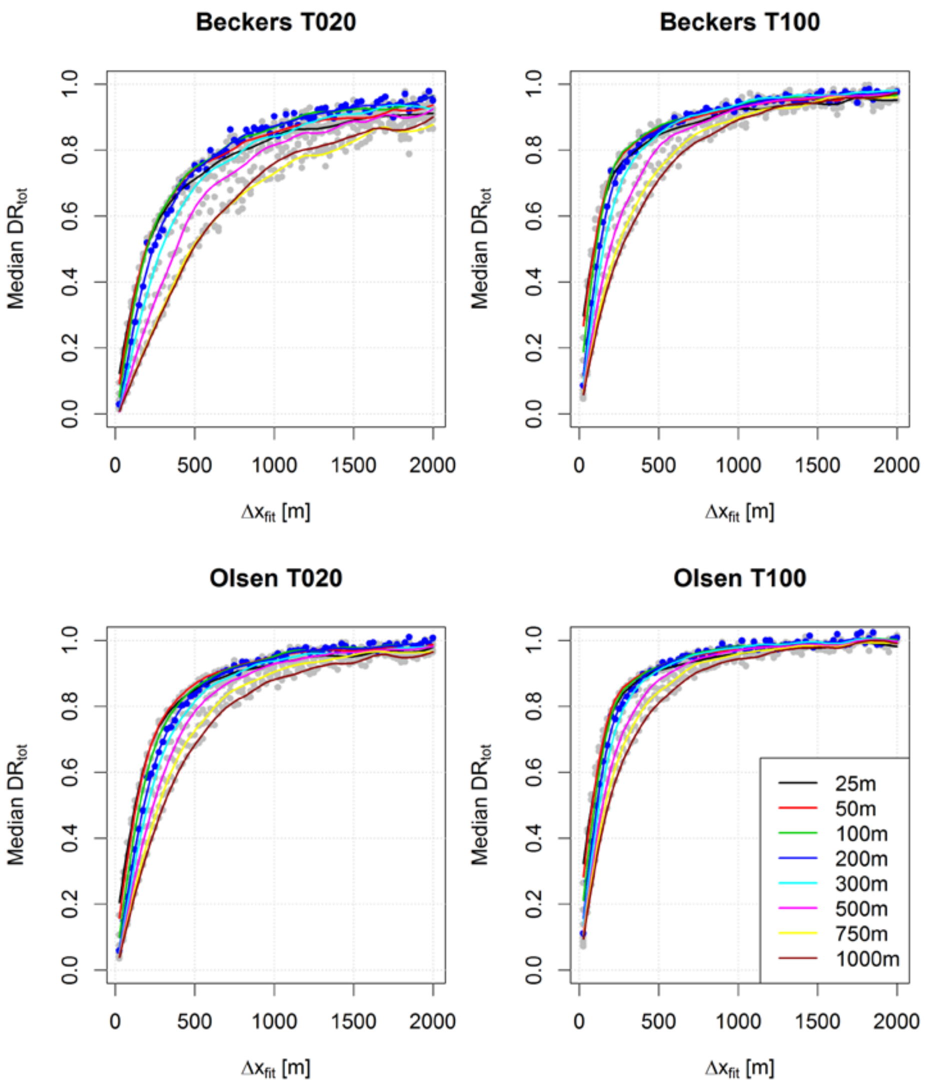

Figure S 6. Median of DR_{tot} obtained during cross validation for flood damage regression models (DMOD1) fitted at different data resolutions Δx_{fit} and considering building data aggregated to different resolutions in m (lines with varying colors). Lines were smoothed while dots indicate the true DR_{tot} values derived for each combination of fitting resolution and building input data resolution. Dots were colored blue for a building data resolution of 200m and grey otherwise.